the pairs of atoms not directly involving in bonding. As expected, these bond orders are quite small.

The covalent bond orders in the acetylene, ethylene, and ethane molecules follow the expectations based on chemical intuition. All the C-H bonds have their P_{AB}'s close to 1, whereas the covalent bond orders of the bonds between the carbon atoms are close to 3, 2, and 1, respectively. The bond orders between the nonbonded pairs of atoms (including the vicinal hydrogen atoms) are again small.

In the course of bond order calculations reported in this paper, we found only one maximum of N_a per molecule, with the obvious exception of the benzene molecule. In accordance with the number and the character of the Kekulé structures, for the benzene molecule, we obtained two identical maxima, with the pattern of covalent bond orders exhibiting symmetry reduced from D_{6h} to $_{D3h}$ (Figure 1). The C-C bonds have the bond orders of ca. 1.2 and 1.6, which averages to ca. 1.4 in the real molecule. The C-H bond orders are close to 1 in both the individual resonance structures and the molecule itself.

The CHF_3 molecule, in which the C-H covalent bond order is considerably smaller than in the unsubstituted hydrocarbons, illustrates nicely the influence of substituents on the ionicity of adjacent bonds. In the CF_3^- anion, the C-F covalent bond orders are slightly larger than in CHF_3.

Our recent calculations on the $CH(CN)_3$ and $C(CN)_3^-$ systems[38] confirmed that, in the latter, the electron delocalization results in stronger C-C bonds and weakened C-N bonds. This conclusion has been drawn from the changes in the optimized bond lengths and the electron densities at the relevant critical points accompanying deprotonation of $CH(CN)_3$. The computed covalent bond orders, displayed in Figure 2a,b, provide even more a transparent manifestation of this effect. In the $CH(CN)_3$ molecule, the C-C bond orders have values close to 1, whereas the magnitudes of the C-N bond orders are very close to those in the HCN molecule. On the other hand, in the $C(CN)_3^-$ anion, the values of P_{AB}'s increase for the C-C bonds and decrease by almost the same amount for the C-N bonds. Quite similar but less dramatic changes are observed in the $C_2(CN)_4$ (TCNE) molecule (Figure 2c) as compared to ethylene. In this case, the electron-withdrawing CN substituents lower the covalent bond order of the central C-C bond considerably.

(38) Cioslowski, J.; Mixon, S. T.; Fleischmann, E. D. *J. Am. Chem. Soc.*, in press.

Conclusions

The proposed definition of the covalent bond order has several advantages over the previously known ones.

First, it does not rely on an explicit assignment of the basis functions to individual atoms. Numerical values of the computed bond orders are quite insensitive to the choice of the basis set, provided the particular basis set is capable of providing an accurate description of the electron distribution in the molecule in question. One should remark that the minimal basis sets (such as STO-3G) are usually inadequate for this purpose as reflected by large errors in the calculated dipole moments and GAPT charges.[24] The covalent bond orders are expected to converge smoothly with increasing number of basis functions to a limit independent of the nature of these functions (multicenter functions, one-center functions, bond functions, ghost orbitals, numerical orbitals, etc.).

Second, the definition follows from a simple partitioning of the total number of electrons present in the molecule under consideration. Minimization of the diatomic term leads to localization of the spin orbitals. The contribution of each localized spin orbital to each atomic pair is then assessed by means of calculating a weighted product of the relevant atomic overlap matrix (AOM) elements. This yields bond orders for individual Lewis (resonance) structures represented by localized spin orbitals. If more than one of such structures exist, a simple averaging provides the covalent bond orders of the real molecule.

Such a prescription results in covalent bond orders that are physically significant, quite easy to calculate, and transparent to interpretation. The presented examples demonstrate that the computed bond orders follow the expectations based on chemical intuition, reproducing for instance the inductive and resonance effects of substituents. The proposed covalent bond orders can be therefore used as companion indices to the Bader atomic charges.

Acknowledgment. This research was partially supported by the National Science Foundation under Contract CHE-9015566 and by the Florida State University through time granted on its CRAY Y-MP supercomputer. J.C. also acknowledges support by the Camille and Henry Dreyfus Foundation New Faculty Award Program.

Ab Initio Study of the Insertion Reaction of Mg into the Carbon-Halogen Bond of Fluoro- and Chloromethane

Steven R. Davis

Contribution from the Department of Chemistry, University of Mississippi, University, Mississippi 38677. *Received December 5, 1990*

Abstract: Theoretical calcuations using self-consistent field (SCF) and Moller-Plessett perturbation theory, up to fourth order (MP4), have been carried out on the gas-phase $Mg + CH_3X \rightarrow CH_3MgX$ Grignard reaction surface for X = F and Cl. The transition-state energies, geometries, and vibrational frequencies for both reactions are presented and compared to the smaller $Mg + HX \rightarrow HMgX$ reaction. The transition states for both X = F and X = Cl are found to possess C_s symmetry and to be almost identical in structure. The activation energy for the Mg + fluoromethane reaction is found to be 31.2 kcal·mol^{-1}, while that for the chloromethane reaction is substantially higher, at 39.4 kcal·mol^{-1}, calculated at the MP4SDTQ level by using the 6-311G(d,p) basis. The intrinsic reaction coordinate has been followed down from the transition state toward both reactants and product for the $Mg + CH_3F \rightarrow CH_3MgF$ reaction, confirming the connection of these points on the potential surface.

Introduction

The reaction of magnesium with fluorocarbons such as tetrafluoroethylene (TFE) has received interest due to its pyrotechnic applications. Formulations involving Mg dispersed in solid TFE burn readily and contain many advantageous characteristics as rocket motor igniters and flares.[1-5] The mechanism of the combustion reaction is not entirely clear,[6,7] and attention is being

(1) Keller, R. B., Ed. *Solid Rocket Motor Igniters*; NASA SP. 8051, March 1971.

0002-7863/91/1513-4145$02.50/0 © 1991 American Chemical Society

focused by using both experimental and theoretical methods to help unravel the kinetics and mechanism of this reaction. In the initial combustion process, the insertion reaction of magnesium into a carbon–fluorine bond to form a Grignard structure is a possible first step. In light of this, we initiated a study of the reaction of Mg atoms with fluoromethane as a preliminary investigation leading to the larger C_2F_4 species.

The reactivity of bare Mg atoms and clusters have received much attention lately as it relates to Grignard chemistry and catalysis processes. Ault[8] reported the formation and spectroscopic characterization of the unsolvated Grignard species H_3CMgX (X = Cl, Br, I) by the matrix isolation technique. The insertion reaction occurred upon codeposition of Mg and CH_3X at 15 K. Interestingly enough, neither photolysis nor annealing of the matrix was required to initiate the reaction. Klabunde et al.[9] studied the reactivity of both main-group and transition-metal atoms under matrix isolation conditions and suggested the possibility that Mg metal clusters play an important role in the Grignard reaction. Additional work revealed evidence for greater reactivity of Mg clusters toward alkyl halides than Mg atoms alone.[10]

Several theoretical articles have appeared in relation to the above-mentioned experimental studies. Sakai and Jordan[11] presented the equilibrium geometry and associated vibrational frequencies of the H_3CMgCl species at the Hartree–Fock level in the 6–31G(d) basis, supporting Ault's[8] spectroscopic characterization of an unsolvated Grignard. In a study relating the importance of magnesium clusters, structural and energetics calculations comparing a dimagnesium Grignard (RMgMgX) with that of a simple one (RMgX) by Jasien and Dykstra[12] showed that there is a 5–6 kcal·mol^{-1} stabilization that arises from the formation of a dimagnesium Grignard from a simple one for HF, CH_3F, and CH_3Cl. However, the disproportionation-like reaction of a dimagnesium Grignard with another alkyl halide to form two Grignards was nearly as exothermic as the formation of a single Grignard. The transition-state geometries and energies for the insertion reaction of Mg and Mg_2 into HF have been reported and found to have comparable activation energies.[13]

There has not been a concomitant study of the Mg insertion reaction into a simple alkyl halide in which the transition state is identified along with a partial characterization of the potential surface. The calculations reported here characterize the transition-state (TS) geometries for the Mg insertion reaction into CH_3F and CH_3Cl to form a Grignard compound. The activation energies at various levels of theory are given, and the intrinsic reaction path along the PES is given. The vibrational frequencies of the reactants, products, and transition states are calculated.

Theoretical Methods

The ab initio calculations were performed by using the Gaussian 86[14] and Gaussian 88[15] series of programs. Several basis sets were used at various levels of theory to ascertain their separate and combined effects on the geometries, relative energies, and vibrational frequencies. Initially the standard 6-31G(d,p) basis was used at the Hartree–Fock level to determine the minima and transition states. The equilibrium geometries were obtained by analytic gradient techniques by using the Berny algorithm.[16] These results were compared to those obtained with a larger basis consisting of the standard Dunning[17] and McLean–Chandler[18] contraction of Huzinaga's[19,20] primitives with one set of d functions added to heavy atoms and a set of p functions added to hydrogen. For carbon and fluorine, this is designated as (9s,5p,1d/4s,2p,1d), with α_d = 0.75 and 0.90, respectively, while for hydrogen it is designated as (4s,1p/2s,1p), with α_p = 1.00. For magnesium and chlorine, the designation is (12s,9p,1d/6s,5p,1d), with α_d = 0.175 and 0.75, respectively. This basis set will be referred to as MC/D95(d,p). The stationary points were characterized as a minimum, transition state (one imaginary frequency) or a higher order saddle point (≥2 imaginary frequencies) by determination of harmonic vibrational frequencies using analtyic second derivatives.[21]

Electron correlation effects were included by using Moller–Plesset perturbation theory through second and fourth order[22] and single reference configuration interaction including all single and double substitutions.[23] Geometries were optimized at the MP2 level with use of analytic gradients[24] with all orbitals active. The basis sets used in these MP2 calculations were the standard 6-31G(d,p)[25] and 6-311G(d,p).[26] For Mg and Cl in the 6-311G(d,p) basis, the McLean–Chandler contraction (12s,9p,1d/6s,5p,1d) is used. Vibrational frequencies were also determined at the MP2 level of theory, with all orbitals active, by numerical differentiation of analytic gradients.[27] Perturbation theory through fourth order, MP4SDTQ, with the core orbitals omitted, was used at the MP2-optimized geometries to calculate energies. Equilibrium geometries were determined at the CID and CISD levels, with all orbitals active, by using analytic gradients.[28]

Table I. Equilibrium Geometries of the Transition State and Activation Energies (E_a) for the Mg + HX → HMgX Reaction

parameter	SCF[b]	ACCD[c,d]	MP2[e]	CID[b,f]	CISD[b,f]
			X = F		
R(H–F)	1.4257	1.520	1.4970	1.4326	1.4311
R(Mg–H)	1.7936	1.985	1.7984	1.7954	1.7966
R(Mg–F)	1.8362	1.834	1.8585	1.8541	1.8569
∠(H–Mg–F)	46.2	47	48.3	46.2	46.1
E_a	55.9	36.5	34.9	50.1 (39.7)	48.9 (37.2)
			X = Cl		
R(H–Cl)	1.7635	1.803	1.7493		
R(Mg–H)	1.8234	1.925	1.8264		
R(Mg–Cl)	2.4931	2.483	2.4167		
∠(H–Mg–Cl)	45.0	46	46.1		
E_a	49.2		32.1		

[a] Bond lengths in angstroms, bond angles in degrees, and energies in kilocalories per mole. [b] Basis is MC/D95(d,p). [c] Taken from ref 13. [d] Basis is (8s4p1d/5s3p1d/4s1p). [e] Basis is 6-311G(d,p). [f] Values in parenthesis corrected for size consistency.

(2) LoFiego, L. Western State Section/The Combustion Institute, Menlo Park, CA, Fall 1968; Paper 68–32.
(3) Robertson, W. E. Am. Inst. Astronautics and Aeronautics, November–December 1972; Paper 72–1195.
(4) Crosby, R.; Mullenix, G. C.; Swenson, I. Am. Inst. Astronautics and Aeronautics, 1972; Paper 72–1196.
(5) Peretz, A. J. *Spacecr. Rockets* **1984**, *21*, 222.
(6) Kubota, N.; Serizawa, C. Am. Inst. Astronautics and Aeronautics, 1986; Paper 86–1592.
(7) Kubota, N.; Serizawa, C. *Propellants, Explos., Pyrotech.* **1987**, *12*, 145.
(8) Ault, B. S. *J. Am. Chem. Soc.* **1980**, *102*, 3480.
(9) Tanaka, Y.; Davis, S. C.; Klabunde, K. J. *J. Am. Chem. Soc.* **1982**, *104*, 1013.
(10) Imizu, Y.; Klabunde, K. *J. Inorg. Chem.* **1984**, *23*, 3602.
(11) Sakai, S.; Jordan, K. D. *J. Am. Chem. Soc.* **1982**, *104*, 4019.
(12) Jasien, P. G.; Dykstra, C. E. *J. Am. Chem. Soc.* **1983**, *105*, 2089.
(13) Jasien, P. G.; Dykstra, C. E. *J. Am. Chem. Soc.* **1985**, *107*, 1891.
(14) Gaussian 86: Frisch, M. J.; Binkley, J. S.; Schlegel, H. B.; Raghavachari, K.; Melius, C. F.; Martin, R. L.; Stewart, J. J. P; Bobrowicz, F. W.; Rohlfing, C. M.; Kahn, L. R.; Defrees, D. J.; Seeger, R.; Whiteside, R. A.; Fox, D. J.; Fluder, E. M.; Pople, J. A. Carnegie-Mellon Quantum Chemistry Publishing Unit: Pittsburgh, PA, 1984.
(15) Gaussian 88: Frisch, M. J.; Head-Gordon, M.; Schlegel, H. B.; Raghavachari, K.; Binkley, J. S.; Gonzales, C.; Defrees, D. J.; Fox, D. J.; Whiteside, R. A.; Seeger, R.; Melius, C. F.; Baker, J.; Martin, R. L.; Kahn, L. R.; Stewart, J. J. P; Fluder, E. M.; Topiol, S.; Pople, J. A. Gaussian, Inc.: Pittsburgh, PA, 1988.
(16) Schlegel, H. B. *J. Comput. Chem.* **1982**, *3*, 214.
(17) Dunning, T. H. *J. Chem. Phys.* **1970**, *53*, 2823.
(18) McLean, A. D.; Chandler, G. S. *J. Chem. Phys.* **1980**, *72*, 5639.
(19) Huzinaga, S. *J. Chem. Phys.* **1965**, *42*, 1293.
(20) Huzinaga, S. *Approximate Atomic Functions II*; Department of Chemistry Report, University of Alberta: Edmonton, Alberta, Canada, 1971.
(21) Pople, J. A.; Krishnan, R.; Schlegel, H. B.; Binkley, J. S. *Int. J. Quantum Chem., Quantum Chem. Symp.* **1979**, *13*, 325.
(22) Krishnan, R.; Pople, J. A. *Int. J. Quantum Chem.* **1978**, *14*, 91.
(23) Pople, J. A.; Binkley, J. S.; Seeger, R. *Int. J. Quantum Chem., Quantum Chem. Symp.* **1976**, *10*, 1.
(24) Pople, J. A.; Krishnan, R.; Schlegel, H. B.; Binkley, J. S. *Int. J. Quantum Chem., Quantum Chem. Symp.* **1979**, *13*, 325.
(25) Franchl, M. M.; Pietro, W. J.; Hehre, W. J.; Binkley, J. S.; Gordon, M. S.; Defrees, D. J.; Pople, J. A. *J. Chem. Phys.* **1982**, *77*, 3654.
(26) Krishnan, R.; Binkley, J. S.; Seeger, R.; Pople, J. A. *J. Chem. Phys.* **1980**, *72*, 650.
(27) Krishnan, R.; Schlegel, H. B.; Pople, J. A. *J. Chem. Phys.* **1980**, *72*, 4654.
(28) Raghavachari, K.; Pople, J. A. *Int. J. Quantum Chem.* **1981**, *20*, 167.

Results and Discussion

This paper deals with the insertion of a Mg atom into the carbon–halogen bond of fluoro- and chloromethane to form the corresponding Grignard reagent according to the following reaction scheme:

$$Mg + H_3CX \rightarrow [H_3CXMg]^{\ddagger} \rightarrow H_3CMgX \qquad X = F, Cl \tag{1}$$

The portion of the potential energy surface connecting the products and reactants will be examined and discussed along with a description of its sensitivity to basis set and level of theory.

Mg + HF. The reaction between both Mg atoms and Mg_2 dimers with HF has been studied previously,[13] and the transition-state (TS) geometries have been located at both the SCF and ACCD (approximate double-substitution coupled cluster)[29,30] methods. Here, we perform calculations on the same system with the various basis sets and methods used in the present study for comparison and to provide a basis for the alkyl halide + Mg system. The equilibrium geometries for the transition states and activation energies determined for the Mg + HF reaction are given in Table I. The H-F bond length shows the greatest deviation between the four methods, being the shortest by using CI and longest at the ACCD level. The MP2 calculated length is closer to the latter method but still shorter by 0.023 Å. The MP2 and CI levels all give a substantially shorter Mg–F bond (0.188 Å on average) than the ACCD method and agree to within 0.003 Å of each other. The Mg–F bond on the other hand is slightly shorter than the ACCD results but by only 0.025 Å for the MP2 level and an average of 0.022 Å for the CI results. The CID and CISD methods agree very well among themselves and give bond lengths and a bond angle to within 0.0012–0.0025 Å and 0.1°, respectively. The H–Mg–F angle is fairly consistent within the four methods, varying by a maximum of 2.2° (MP2 vs CISD). The H–F bond in the TS is lengthened relative to free H–F by about 56–64%, depending on the computational level.

Activation energies for the insertion reaction agree well within the four methods. The difference between the ACCD and MP2 results is just 1.6 kcal·mol^{-1}. The two CI activation energies are close to each other (2.5 kcal·mol^{-1}) but are significantly higher than the other two levels, presumably due to truncated CI not being size-consistent. However, when corrected for size consistency,[31] the values fall to within 4.8 and 2.3 kcal·mol^{-1} of the MP2 value for the CID and CISD methods, respectively. For the Mg reaction with HCl, the activation energy has been reported to be approximately 10 kcal·mol^{-1} less than that for HF at both the SCF and ACCD methods.[13] Using the MC/D95(d,p) basis, we find a difference of 6.7 kcal·mol^{-1} at the SCF level and a smaller gap of 2.8 kcal·mol^{-1} at the MP2 level within the 6-311G(d,p) basis.

In summary, the bond lengths at the CID and CISD levels of theory are consistently shorter than those obtained from the MP2 calculations, and with the exception of the Mg–F bond distance the ACCD bond lengths are longer than those obtained from the other three methods. With only one exception, however (Mg–H length), all bond lengths are within a few hundredths of an angstrom when compared to those obtained from another calculational method. As far as activation energies are concerned, all four methods give values remarkably close to each other as long as a size-consistency correction is applied to the truncated configuration interaction energies. From this comparison, we fell that meaningful results can be obtained for the larger Mg + CH_3F and CH_3Cl systems and will restrict the calculation of correlation effects to the MP2 and MP4 techniques.

CH_3MgF and CH_3MgCl. Ab initio calculations of the Grignard complexes CH_3MgF and CH_3MgCl have been reported in the literature previously. The equilibrium geometry for the CH_3MgF molecule has been calculated at the SCF level, but the C–H length and H–C–Mg angle were each held constant.[13,32] A total optimization in C_{3v} symmetry has been reported, along with vibrational frequencies, for CH_3MgCl[11] at the SCF level using the 6-31G(d) basis. We have performed a full optimization (within the C_{3v} point group) at both the SCF and correlated levels, and the geometrical parameters are given in Table II. The C–H bond lengths and C–H–X angles are virtually identical going from CH_3MgF to CH_3MgCl at each level of theory. The C–Mg bond is consistently shorter by a small margin in the CH_3MgCl molecule than in its fluorine counterpart. However, the partial charge on each atom as determined by a Mulliken population analysis is found to be extremely sensitive to the basis set employed. The charges found at the optimized structure for each basis set are given in Table III. The MC/D95 basis consistently gave greater atomic charges than did the 6-31G(d,p) basis. For CH_3MgF, the carbon atom has acquired −0.42 au of charge from the three hydrogens plus −0.39 au from the Mg atom in the MC/D95 basis. The Mg has lost 1.07 electrons, while F has gained −0.69, making both the Mg–F and C–Mg bonds somewhat ionic in character. The charges are less in magnitude at the 6-31G(d,p) level, with the most dramatic change in the carbon and hydrogen atoms. However, the Mg–F bond still contains a fair amount of ionic character. For CH_3MgCl, the charge separation in the Mg–Cl and C–Mg bonds are greatly reduced in the 6-31G(d,p) basis

Table II. Equilibrium Geometries for the Grignard Molecules CH_3MgF and CH_3MgCl in C_{3v} Symmetry[a]

parameter	SCF[b,c]	SCF[d]	MP2[e]
	CH_3MgF		
R(C–Mg)	2.080	2.0917	2.0848
R(Mg–F)	1.779	1.7524	1.7775
R(C–H)	1.09	1.0888	109.46
∠(H–C–Mg)	109.5	111.54	111.41
energy	−338.7047	−338.755 07	−339.323 47
	CH_3MgCl		
R(C–Mg)	2.090	2.0853	2.0799
R(Mg–Cl)	2.217	2.2116	2.1987
R(C–H)	1.088	1.0887	1.0947
∠(H–C–Mg)	111.7	111.56	111.46
energy	−698.764 95	−698.814 75	−699.338 04

[a] Units in angstroms, degrees, and hartrees for bond lengths, bond angles, and energies, respectively. [b] CH_3MgF results taken from ref 32. [c] CH_3MgCl results taken from ref 11. [d] Basis is MC/D95(d,p). [e] Basis is 6-311G(d,p).

Table III. Net Atomic Charges (au) from Mulliken Population Analysis for the Grignard Complexes and Transition States

C	H	H′	Mg	F	Cl	basis
			CH_3MgF			
−0.808	0.141		1.070	−0.685		MC/D95(d,p)
−0.625	0.112		0.934	−0.645		6-31G(d,p)
			CH_3MgCl			
−0.818	0.143		0.911		−0.522	MC/D95(d,p)
−0.636	0.116		0.672		−0.384	6-31G(d,p)
−0.81	0.17		0.69		−0.38	6-31G(d)[a]
			$CH_3FMg^{\ddagger}$			
−0.254	0.203	0.216	0.256	−0.637		MC/D95(d,p)
−0.208	0.207	0.207	0.152	−0.564		6-31G(d,p)
			$CH_3ClMg^{\ddagger}$			
−0.316	0.216	0.217	0.107		−0.440	MC/D95(d,p)
−0.274	0.225	0.219	0.022		−0.410	6-31G(d,p)

[a] Taken from ref 11.

(29) Chiles, R. A.; Dykstra, C. E. *Chem. Phys. Lett.* **1981**, *10*, 69.
(30) Jankowski, K.; Paldus, J. *Int. J. Quantum Chem.* **1980**, *18*, 1243.
(31) Pople, J. A.; Seeger, R.; Krishnan, R. *Int. J. Quantum Chem., Quantum Chem. Symp.* **1977**, *11*, 149.
(32) Baskin, C. P.; Bender, C. F.; Lucchese, R. R.; Bauschilder, C. W.; Schaefer, H. F. *J. Mol. Struct.* **1976**, *32*, 125.

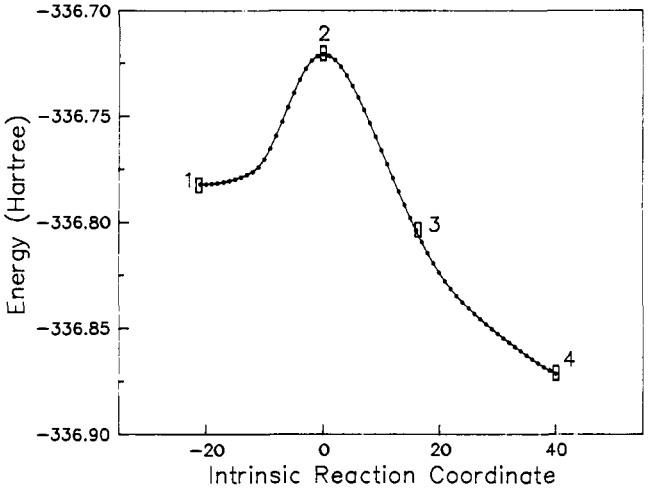

Figure 1. Potential energy profile along the reaction surface for Mg + $CH_3F \rightarrow CH_3MgF$ at the HF/3-21G(d) level. The zero point along the reaction coordinate is the TS with reactants toward the negative direction and products toward the positive direction.

although the MC/D95 calculations still show substantial ionic character for both the C–Mg and Mg–Cl bonds.

The overall energetics of the Mg + $CH_3X \rightarrow CH_3MgX$ reaction has been calculated previously at various levels of theory. At the SCF level, the reaction exothermicities[13] are 42.8 and 53.7 kcal·mol^{-1} for fluoromethane and chloromethane, respectively. At the MP2/6-311G(d,p)//MP2/6-311G(d,p) level, the two are 55.7 and 54.4 kcal·mol^{-1}, respectively.

Mg + CH_3F. The insertion reaction of a Mg atom into the C–F bond of CH_3F was studied and the transition state located at the SCF and correlated levels of theory. This point on the potential energy surface was characterized by calculation of the harmonic force constants, which resulted in one imaginary frequency. However, it is not always clear from the normal coordinate of the imaginary frequency that the transition state is one that connects the desired reactants and products. This is due to that fact that the harmonic approximation is valid for only very small displacements. Therefore, we followed the potential energy surface in both directions down from the transition state along the intrinsic reaction coordinate (IRC). The results are shown in Figures 1 and 2, which show that the located saddle point indeed connects the isolated Mg and CH_3F moieties with the CH_3MgF Grignard structure. The optimized geometries at various points on the reaction potential surface are shown in Figure 2. The calculation down from the TS came very close to reaching the initial reactants and the final Grignard product, but as the slope of the potential along the IRC became close to zero (at the reactants and product) the search routine had difficulty locating the next point. However, it is easily seen that the desired reactants and product do lie on the IRC surface. The sequence from reactants to transition state starts with an interaction of Mg with the fluorine atom of the CH_3F molecule. This interaction quickly progresses, yielding a relatively short Mg–F distance of 1.83 Å in the TS. Upon the initial interaction of the two moieties, the Mg–F–C bond angle decreases as the Mg atom moves closer to the carbon atom. However, in the TS, the C–Mg length is still somewhat long at 2.64 Å. The hydrogen atoms can be observed becoming tetrahedral around the C–Mg bond as this distance decreases. As the reaction proceeds from the TS to products, the C–F bond is ruptured, the C–Mg distance decreases, and the C–Mg–F angle increases from 89 to 180°.

Table IV. Equilibrium Geometries of the Transition State for the Mg + $CH_3X \rightarrow CH_3MgX$ Reaction[a] (X = F, Cl)

	X = F		X = Cl	
parameter	SCF[b]	MP2[c]	SCF[b]	MP2[c]
R(C–Mg)	2.8066	2.6382	2.9862	2.7471
R(C–X)	2.0460	1.8668	2.5174	2.2554
R(Mg–X)	1.8277	1.8828	2.3920	2.3811
R(C–H)	1.0729	1.0811	1.0693	1.0839
R(C–H′)	1.0703	1.0843	1.0724	1.0843
∠(Mg–C–X)	40.58	45.53	50.65	55.81
∠(H–C–X)	121.04	84.40	77.80	84.13
∠(H′–C–X)	85.05	111.89	106.29	113.32
∠(H′–C–X–H)	120.27	114.56	116.42	113.05
∠(Mg–C–X–H)	0.00	180.0	180.0	180.0
energy	−338.603 54	−339.179 67	−698.649 63	−699.182 37

[a] Units in angstroms, degrees, and hartrees for bond lengths, bond angles, and energies, respectively. The angle ∠(A–B–C–D) represents the dihedral angle formed between the A–B–C and B–C–D planes. [b] Basis is MC/D95(d,p). [c] Basis is 6-311G(d,p).

The geometrical parameters and energies of the transition state are given in Table IV, while the MP2-optimized structure is shown pictorially in Figure 3. The transition state is found to have C_s symmetry, with the Mg–C–F plane bisecting an H–C–H angle. The C–F bond is lengthened by 0.49 Å (35%) compared to that in CH_3F, while the C–Mg bond is 0.55 Å (27%) longer than that is the CH_3MgF Grignard molecule. The Mg–F distance is remarkably close to the Mg–F bond distance in the Grignard structure, being only 0.11 Å (5.9%) longer. In consequence, there appears to be a greater amount of bonding between the Mg and F atoms than between Mg and C in the TS. Part of this could arise from electrostatic attraction between the F and Mg, which carry opposite partial charges. There are only slight changes in the C–H bond distances, and they are of no real consequence. However, the H–C–F and H′–C–F angles have changed substantially in the TS. The greatest being that for H′ for which a value of 84.4° is obtained. Here, H′ refers to the hydrogen atom in the C_s symmetry plane. As a bond is formed between the C and Mg, a tetrahedral arrangement containing this new bond is accomplished. The H′–C–Mg angle of 130° is intermediate between a true tetrahedral arrangement about either the C–F or C–Mg bonds. For H′–C–Mg, the value is approximately 20° greater than tetrahedral, while for H–C–Mg it is 20° less. The angle for the other two hydrogens (symmetrically equivalent) is 89.2° for H–C–Mg and 111.9° for H–C–F. As the intrinsic reaction coordinate is followed from the TS to the product

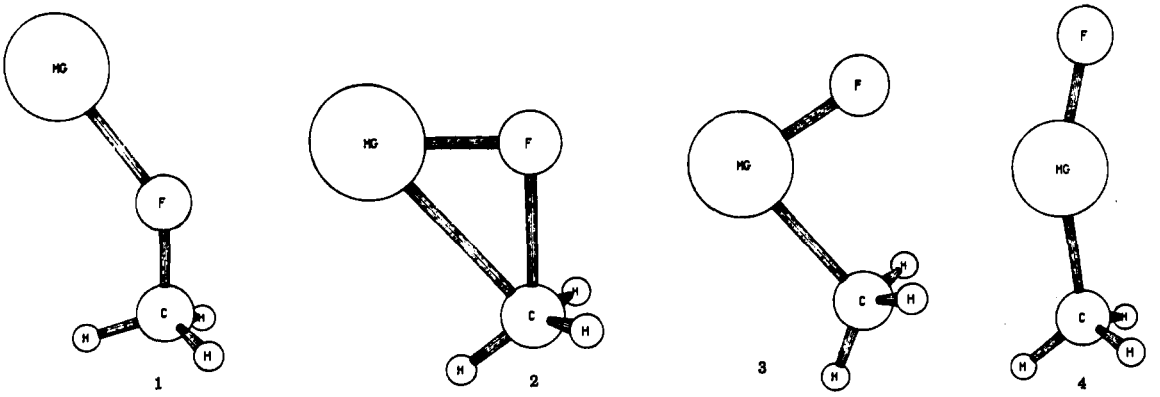

Figure 2. Optimized geometries for selected points along the intrinsic reaction coordinate calculated at the HF/3-21G(d) level. See Figure 1 for selected points.

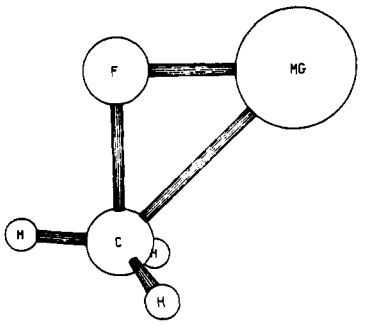

Figure 3. Transition-state structure for Mg + $CH_3F \rightarrow CH_3MgF$ optimized at the MP2/6-311G(d,p) level.

(Grignard structure), these two angles tend smoothly toward a tetrahedral value containing the C–Mg bond.

One interesting result is the sensitivity of the dihedral angle, made by the two planes Mg–C–F and C–F–H, to the effects of electron correlation. At the SCF level with use of the 3-21G(d), 6-31G(d,p), and the MC/D95(d,p) basis, the value of this dihedral angle is found to be 0°. At the correlated level with use of the 6-31G(d,p) and 6-311G(d,p) basis sets, the dihedral angle becomes 180°. Also, if the geometry is optimized at the MP2 level with the dihedral angle constrained to be 0°, two imaginary frequencies are obtained. A 785i cm^{-1} frequency corresponds to the reaction coordinate (747i in the TS), while the smaller magnitude 112i cm^{-1} frequency corresponds to displacement about the dihedral angle. Analogous results are obtained at the SCF level except that a dihedral angle of 180.0° gives two imaginary frequencies, a greater magnitude one (541i cm^{-1}) along with a smaller 64i cm^{-1} frequency describing displacement about the dihedral angle. The smallest magnitude vibrational frequency for the TS and second-order saddle points shows that the potential surface describing motion about the dihedral angle is very shallow for the TS and only slightly raised, by 0.7 kcal·mol^{-1}, for the second-order saddle point.

The net atomic charges for the transition-state structure show the intermediate nature of the C–Mg and Mg–F bonds. The F atom gains electron density mostly through the carbon atom, while the Mg atom is only slightly positive. The carbon atom contains much less excess charge here than in the Grignard molecule (due to the C–F interaction), while the hydrogens are more charged due to the withdrawing tendency of the fluorine atom. The extent of the insertion can be correlated with the partial charge on the magnesium atom. The Mg loses electron density upon bond formation with C and F until a somewhat ionic bond is formed in the Grignard structure. The carbon, magnesium, and fluorine atoms contain a greater magnitude of charge in the MC/D95 basis, which suggests a greater extent of reaction.

The activation energy for the insertion reaction is found to be 51.6 kcal·mol^{-1} at the SCF/MC/D95(d,p) level and 33.3 kcal·mol^{-1} for the MP2/6-311G(d,p) calculation. The inclusion of electron correlation lowers the activation energy by a substantial amount, as was seen with the Mg + HF reaction. The activation energy is only slightly lower (1.6 kcal·mol^{-1}) for the Mg reaction with CH_3F than for hydrogen fluoride at the MP2 level.

The harmonic vibrational frequencies are given in Table V. The magnitude of the imaginary frequency increases substantially upon inclusion of electron correlation due to the increased curvature of the potential surface at this point. The lowest real frequency, largely a hydrogen bending motion about the Mg–C–F–H dihedral angle, also increases in magnitude by a large extent. The other low frequencies (below 1000 cm^{-1}) increase in magnitude with the inclusion of electron correlation, while the higher ones decrease as expected. The two highest modes, one a C–H′ (a′) and the other a C–H stretch (a″), switch due to correlation effects.

Mg + CH_3Cl. The Grignard reaction between Mg and CH_3Cl was studied and compared to the results obtained with CH_3F. Geometric results for the TS are given in Table IV, and the structure is shown in Figure 4. The Mg–C–Cl–H dihedral angle

Table V. Vibrational Frequencies (cm^{-1}) for the $CH_3XMg^{\ddagger}$ Transition States

$CH_3FMG^{\ddagger}$				$CH_3ClMg^{\ddagger}$			
SCF	irrep	MP2	irrep	SCF	irrep	MP2	irrep
583i	a′	747i	a′	506i	a′	876i	a′
12	a″	103	a″	70	a″	148	a″
251	a′	258	a′	193	a′	203	a′
571	a′	556	a′	308	a′	346	a′
672	a′	684	a″	641	a″	667	a″
788	a″	835	a′	720	a′	747	a′
1155	a′	1097	a′	1137	a′	1093	a′
1541	a′	1465	a′	1530	a′	1452	a′
1553	a″	1472	a″	1547	a″	1465	a″
3228	a′	3156	a′	3323	a′	3155	a′
3512	a′	3303	a″	3512	a″	3290	a′
3531	a″	3311	a′	3527	a′	3306	a″

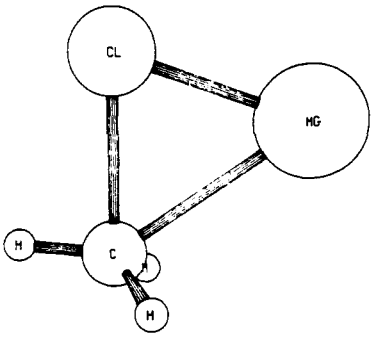

Figure 4. Transition-state structure for Mg + $CH_3Cl \rightarrow CH_3MgCl$ optimized at the MP2/6-311G(d,p) level.

of 180.0° in the transition state is found to be the same at both the SCF and MP2 levels, in contrast to that found for the $CH_3FMg^{\ddagger}$. Therefore, both the $CH_3FMg^{\ddagger}$ and $CH_3ClMg^{\ddagger}$ transition states have analogous structures at the MP2 level, belonging to the C_s point group. The following comparisons between the two TS structures will be for that calculated at the MP2 level. The C–Mg bond length is slightly longer by 0.11 Å in the $CH_3ClMg^{\ddagger}$ transition state than that above for $CH_3FMg^{\ddagger}$, while the C–H bond lengths are the same to within a few thousandths of an angstrom. The C–Cl and Mg–Cl bonds are necessarily longer due to the larger size of the Cl atom. The H–C–Cl angle is within 0.4° of that in $CH_3FMg^{\ddagger}$ and the H′–C–Cl angles are only 0.56° different. The H′–C–X–H dihedral angles are also about the same (only 1.5° difference). Again, H′ refers to the hydrogen atom in the C_s symmetry plane. The Mg–Cl bond distance in the transition state is farily close to its value in the CH_3MgCl Grignard structure, indicative of a strong interaction between these two atoms.

It is interesting that the bond distances and angles in $CH_3FMg^{\ddagger}$ and $CH_3ClMg^{\ddagger}$ are so similar considering the weaker nature of the C–Cl bond. It might be expected that the lower carbon–halogen bond strength would shift the transition state somewhat. If the degree of reaction is measured by the deviation of the H(H′)–C–Cl angles from tetrahedral, about the Cl atom, the TS states for the two cases are essentially identical. The most pronounced difference though is the longer C–Mg bond in the $CH_3ClMg^{\ddagger}$ molecule, suggesting a slight shift toward reactants.

The vibrational frequencies are given in Table V, and as with the $CH_3FMg^{\ddagger}$ molecule the frequencies below 1000 cm^{-1} increase with the inclusion of electron correlation, while those higher are reduced. The two highest frequencies corresponding to a C–H′ (a′) or C–H stretch (a″) also switch places with the inclusion of electron correlation.

One of the most interesting results is the higher activation energy for the Mg + CH_3Cl reaction. It is well-known that, in solution, the Grignard reaction proceeds more readily, for a particular RX molecule, as X varies from F to I. This is a result of the decreasing R–X bond dissociation energy for the series F > Cl > Br > I. However, the calculations reported here suggest deviant behavior for CH_3X (X = F, Cl) in an isolated gas-phase

Table VI. Activation Energies for the Mg + $CH_3X \rightarrow CH_3MgX$ Reaction (kcal·mol^{-1})

moiety	SCF[a]	SCF[b]	MP2[a]	MP2[c]	MP4SDQ[c]	MP4SDTQ[c]
X = F	49.5	51.6	28.5	33.3	35.7	31.2
X = Cl	54.3	53.2	41.7	42.7	42.1	39.4

[a] Basis is 6-31G(d,p). [b] Basis is MC/D95(d,p). [c] Basis is 6-311G-(d,p).

environment. At the SCF level, the activation energies are within 1.6 kcal·mol^{-1} of each other, but at the MP2 level with use of the 6-311G(d,p) basis, E_a is calculated to be 41.7 kcal·mol^{-1} for Mg + CH_3Cl but only 33.3 kcal·mol^{-1} for Mg + CH_3F (Table VI). The inclusion of electron correlation substantially lowers the activation energy for both, but the magnitude of the correction is almost twice that for the Mg + CH_3F reaction as for Mg + CH_3Cl.

This anomalous behavior, however, is not manifest for the calculated activation barriers for the smaller Mg + HX system. The activation energy is higher for the Mg + HF reaction at both the SCF and correlated levels. Previous calculations by Jasien and Dykstra[30] report a 9–10 kcal·mol^{-1} lower barrier height for HCl at both the SCF and ACCD levels. Calculations using the slightly different basis reported here show a 7 and 3 kcal·mol^{-1} lower barrier for HCl at the SCF and MP2 levels, respectively. The inclusion of electron correlation lowers the activation energies by a relatively similar amount for both X = F and Cl, contrary to that found for the methyl halide case.

In solution, the Grignard reaction is widely recognized as following a mechanism involving free radicals,[33-37] and the magnesium metal surface is reported to play a major role.[38] One mechanism recently proposed is that of Walborsky[38] in which the insertion of Mg into a carbon–halide bond proceeds at the metal surface through three possible schemes. One is through the formation of a radical anion–cation pair in which the C–X bond accepts an electron from the metal into the antibonding orbital to produce an $(RX^{\bullet})^{-}$ radical anion in close proximity with a magnesium cation. The collapse of the radical ion pair results in the formation of the Grignard reagent with retention of configuration. Conversely an R$^{\bullet}$, $^{\bullet}$MgX radical pair can be formed either by separation of the ion pair or by a direct mechanism on the surface. The R$^{\bullet}$ radical can then undergo racemization. Finally, upon combination of the radical pair, the Grignard reagent is formed. The amount of observed racemization has been correlated with the C–X bond strength. The lower the bond energy the more likley a radical pair can be formed by rupture of the C–X bond. Also, the reduction potential of the halogen atom decreases with the C–X bond energy, lessening the probability of the radical ion pair.

In this study, however, the gas-phase mechanism is found to proceed through direct insertion of the Mg atom into the C–X bond without radical ion pair or radical–radical pair intermediacy. However, important differences in the reaction environment are present. The reaction is between a Mg atom and the methyl halide as opposed to a metal cluster, and solvent effects are completely absent. This gas-phase mechanism is supported by the atomic charges obtained in a Mulliken population analysis for the transition state (Table III). The bonding is mostly covalent with slight ionic character.

An experimental study was performed by Ault[8] in which Mg metal was codeposited with CH_3X (X = Cl, Br, I) in an argon matrix with subsequent formation of the unsolvated Grignard molecule CH_3MgX. If the gas-phase reaction proceeded through a radical pair as in solution, it would have been likely that separation of the radicals could occur in these matrix experiments, allowing the individual methyl radical to be trapped in the matrix. The observation of this radical however, was not reported. It was observed that a greater amount of product was obtained with X = Br and I than for X = Cl, supporting the premise that the activation energy is lower for the weaker C–X bonds. However, CH_3F was not included in this study, and it would be interesting, in light of these theoretical results, to determine the extent of reaction for this species. It should be noted that theoretical results obtained for the Mg insertion reaction with vinyl halides also give a lower activation energy for X = F than for X = Cl.[39]

Conclusions

The insertion reaction of Mg into the C–X bond of fluoromethane and chloromethane was studied at the SCF and correlated levels of theory. The transition state for the insertion reaction was located and characterized by the existence of a single imaginary harmonic frequency. To ensure that the located transition state actually connects the isolated Mg + CH_3F with the Grignard structure CH_3MgF, the intrinsic reaction coordinate was followed down from the transition state toward the reactants and product. The transition state for both reactions have very similar geometries and both have C_s symmetry. A strong interaction between the Mg and halogen atom is observed as witnessed by the Mg–X bond being elongated by an average of only 4% in the transition states at the MP2 level. The C–Mg bond is an average of 29% longer in the transition states, however. The H–C–X bond angles are intermediate between being tetrahedral around either the C–F or C–Mg bond, giving evidence of the bonding interaction between C and Mg. Upon following the reaction coordinate toward products, these angles smoothly go to a tetrahedral arrangement about the C–Mg bond.

At the MP2 level with use of the 6-311G(d,p) basis, the activation energies for the insertion reaction was found to be 33.3 and 41.7 kcal·mol^{-1} for Mg + fluoromethane and chloromethane, respectively. These energies decrease only slightly at the MP4SDTQ level to 31.2 and 39.4 kcal·mol^{-1}, respectively. The much lower barrier height for the Mg + CH_3F reaction was surprising in the light of the stronger C–F bond. This behavior was not observed for the Mg insertion reaction with HF and HCl. The barrier heights for this smaller system are more in line with the H–X bond strength, with the Mg + HF reaction having an activation energy 3 kcal·mol^{-1} larger than that for HCl at the MP2 level of theory. In light of Ault's matrix isolation experiments with CH_3X (X = Cl, Br, I), it would be interesting to include fluoromethane and compare the extent of reaction with the other halomethanes as well as the hydrogen halides to shed more light on the activation barrier of the gas-phase Mg + CH_3F reaction.

Acknowledgment. I gratefully acknowledge financial support of this research from the Office of Naval Research under Contract N00014-89-J-2012 and the Mississippi Center for Supercomputing Research.

(33) Karasch, M. S.; Reinmuth, O. *Grignard Reactions of Non-Metallic Substances*; Prentice Hall: New York, 1954.
(34) Gomberg, M.; Bachman, W. E. *J. Am. Chem. Soc.* **1927**, *49*, 236.
(35) Ashby, E. C. *Q. Rev., Chem. Soc.* **1967**, *21*, 259.
(36) Walborsky, H. M.; Young, A. E. *J. Am. Chem. Soc.* **1961**, *83*, 2595.
(37) Grootveld, H. H.; Blomberg, C.; Bickelhaupt, F. *Tetrahedron Lett.* **1970**, 1999.
(38) Walborsky, H. H. *Acc. Chem. Res.* **1990**, *23*, 286.
(39) Liu, L.; Davis, S. R. *J. Phys. Chem.*, in press.